23rd ABCM International Congress of Mechanical Engineering
December 6-11, 2015, Rio de Janeiro, RJ, Brazil

IDENTIFICATION OF AXIAL LOADS APPLIED TO SUBMERSED STRUCTURE BASED ON DYNAMIC RESPONSES

Sigeo Kitatani Jr.
Universidade Federal de Goiás - Avenida Universitária, nº1488, Qd. 86, Bloco A, 3ºandar, Setor Leste Universitário, Goiânia-GO, Brazil, Zip Code 74605-010, P.O. Box 131
sigeojr@ufg.br

Daniel Alves Castelo
Department of Mechanical Engineering, Federal University of Rio de Janeiro (Poli/COPPE), Avenida Um, sem número, Ilha do Fundão, Rio de Janeiro-RJ, Brazil, P.O. Box 68005, Zip Code 21945-970
castello@mecanica.coppe.ufrj.br

Domingos Alves Rade
Technological Institute of Aeronautics, Division of Mechanical Engineering - Praça Mal. Eduardo Gomes, nº50, São José dos Campos-SP, Brazil, Zip code 12228-900
domingos@ita.br

Abstract. *In the present paper it is proposed and evaluated, both numerically and experimentally, an inverse procedure for the indirect determination of axial loads applied to submersed pipe-like structures, based on their dynamic responses. The study is motivated by the existence of practical problems encountered in the oil industry. An experimental test rig has been designed and built, consisting in a reservoir inside which a tubular stainless steel beam has been mounted and tested. Special fixtures have been designed in such a way to enable to apply controlled axial loads and represent different types of boundary conditions. In parallel, computational routines have been developed for the two-dimensional modelling of the structure accounting for the effects of axial loads, flexible supports and fluid-structure interaction, based on the finite element approach. Numerous scenarios have been considered using either numerically simulated or experimentally measured responses. As for the resolution of inverse problem, two strategies has been investigated: the first consist in the deterministic resolution of a constrained optimization problem based on evolutionary algorithms, and the second, which enables to account for the presence of uncertainties in the experimental data, is a stochastic approach based on Bayesian inference, combined with Markov chains and Metropolis-Hastings algorithm. The results obtained confirm the operational feasibility and satisfactory accuracy provided by the suggested identification approaches.*

Keywords: *Fluid-structure interaction, parameter identification, inverse problem, bayesian inference*

1. INTRODUCTION

In the realm of structural engineering, to know external loading is very important, to evaluate the level of security of structures in real service conditions. It is known that stress state of a structure can influence the static and dynamic behavior of structural systems, and this effect is so called *stress-stiffening* (Greening and Lieven, 1999). However, the determination of external loading is not trivial from experimental point of view. To take measurements in operation conditions can incurs in many operational difficulties, as the environment conditions (conditions under which the sensors are subjected), the access to structural elements of structural, etc. In some cases transducers sensors must be installed during construction of the structure.

In these situations, many efforts are employed to estimate lifetime of structures. By taking in account the influence of external loading on the dynamical response of the mechanical system, it is possible to make an inference about the loading, through an inverse problem approach. The inverse problem can be made comparing the experimental dynamic response with responses obtained numerically. Since the dynamic responses represent the global characteristics of the structures, the loading identification can be done through simple measurements in various points along the structure.

In the present work both, deterministic and a Bayesian approaches are used to determines the axial load applied to a submerged beam-like structure. For the modelling of the stress-stiffening effect, a geometric stiffness matrices was used (Flores, 2004). The effect of fluid-structure interaction is proposed as Pavanello (1991), considering a structural acoustic problem. At this scenario, the deterministic inverse problem is done soving a constrained optimization problem in which the cost function is given by the differences between predicted and observed modal properties (Flores *et al.*, 2007). To deal with many sources of uncertainty, presents in physical systems, a Bayesian statistical approach is employed to derive both point estimates and probability distribution for the unknown parameters (e.g., the axial load).

The paper is organized as follows. In the section 2 one describes the modelling of stress-stiffening and fluid-structures effects. In section 3 one describes deterministic inverse problem approach; and in section 4 one describes statistical inverse problem solutions. Finnaly, in section 5, one discribes the physical system under investigation, the forward model, the strategy to generate the simulated experimental data and the estimates for the unknown parameters obtained with a deterministic and Bayesian inference approaches.

2. Fluid-Structure interaction including stress-stiffening effect

In the present work an optimization-based inverse procedure is used for the estimation of axial loads applied to pipelines (used in oil industry), by using information concerning the dynamical behavior of the mechanical system and its corresponding finite element model.

For this purpose, the stress-stiffening effect and fluid-structure interaction (FSI) formulations are presented above.

2.1 Stress-Stiffening effect

For the computational analysis, the mechanical system is modeled using a two-dimensional beam-like structure, according to the theory of Euller-Bernoulli, including the effect of the axial load (Craig Jr, 1981), as illustrated in Fig. 1, where u_i^L and u_i^R are the transversal nodal displacements; θ_i^L and θ_i^R are the nodal cross section rotations; and l_i is the length of the element. For the discrete model,

$$[\mathbf{M}]\{\ddot{\mathbf{X}}(t)\} + [\mathbf{K}(\mathbf{N})]\{\mathbf{X}(t)\} = \mathbf{F}(t), \tag{1}$$

governs the free vibration of the undamped system, where $\mathbf{N}$ is the vector of axial loads applied to the beam elements nodes, that form the finite element model of the structure; $\ddot{\mathbf{X}}$ and $\mathbf{X}$ are vector of accelerations and displacements, respectively, at the system degrees of freedom.

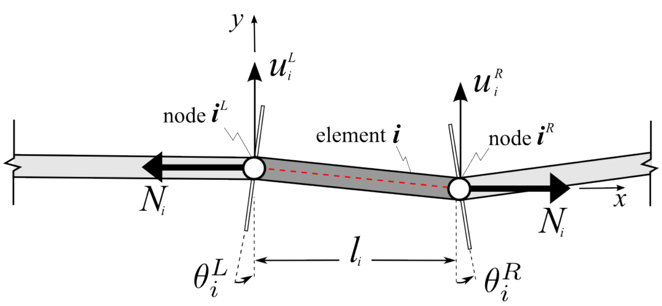

Figure 1. Two-dimentional beam element.

Using linear interpolation function to represent the longitudinal displacement and a cubic function for the transversal displacement (Craig Jr and Kurdila, 2006), the stiffness matrix $[K]$ and the mass matrix $[M]$ are defined as

$$[\mathbf{K}_i] = \left[\mathbf{K}_i^S\right] + \left[\mathbf{K}_i^G\right], \tag{2}$$

$$\left[\mathbf{K}_i^S\right] = \begin{bmatrix} \frac{E_iA_i}{l_i} & 0 & -\frac{E_iA_i}{l_i} & 0 & 0 & 0 \\ & 12\frac{E_iI_i}{l_i^3} & 6\frac{E_iI_i}{l_i^2} & 0 & -12\frac{E_iI_i}{l_i^3} & 6\frac{E_iI_i}{l_i^2} \\ & & 4\frac{E_iI_i}{l_i} & 0 & -6\frac{E_iI_i}{l_i^2} & 2\frac{E_iI_i}{l_i} \\ & & & \frac{E_iA_i}{l_i} & 0 & 0 \\ & & & & 12\frac{E_iI_i}{l_i^3} & -6\frac{E_iI_i}{l_i^2} \\ sim & & & & & 4\frac{E_iI_i}{l_i} \end{bmatrix}, \tag{3}$$

$$\left[\mathbf{K}_i^G\right] = \begin{bmatrix} 0 & 0 & 0 & 0 & 0 & 0 \\ & \frac{6}{5}\frac{N_i}{l_i} & \frac{N_i}{10} & 0 & -\frac{6}{5}\frac{N_i}{l_i} & \frac{N_i}{10} \\ & & \frac{12N_il_i}{5} & 0 & -\frac{N_i}{10} & -\frac{N_il_i}{10} \\ & & & 0 & 0 & 0 \\ & & & & \frac{6}{5}\frac{N_i}{l_i} & -\frac{N_i}{10} \\ sim & & & & & \frac{12N_il_i}{5} \end{bmatrix}, \tag{4}$$

$$
[\mathbf{M}_i] = \frac{m_i}{420}\begin{bmatrix} 140 & 0 & 0 & 70 & 0 & 0 \\ & 156 & 22l_i & 0 & 54 & -13l_i \\ & & 4{l_i}^2 & 0 & 13l_i & -3{l_i}^2 \\ & & & 70 & 0 & 0 \\ & & & & 156 & -22l_i \\ sim & & & & & 4{l_i}^2 \end{bmatrix}, \tag{5}
$$

where E_i is the modulus of elasticity of the material; A_i is the area of the cross section; I_i is the second moment of area; $m_i = \rho_i A_i l_i$ and ρ_i represents the density of the material. The system stiffness matrix is assembled from element stiffness matrices ($\mathbf{K}_i^S$) and geometric stiffness matrices ($\mathbf{K}_i^G$), accounting for the effect of the axial load on the beam element (Livingston *et al.*, 1995), representing the so called *stress-stiffening* effect.

2.2 Structural acoustic problem

In the present work one is concerned with the prediction of the dynamic response of a submersed elastic piping system, used in oil industry. In this situation, the structure is submerged in fluid (water), heavy enough to influence structural response, so that a two-way coupling is required (Felippa and Geers, 1988; Felippa and Park, 2006, 2008). The fluid is treated as a compressible, inviscid, irrotational, isotermic and nonflowing medium whose pressure satisfies the wave equation. For this situation, the principle of conservation of mass and the principle of momentum are given by

$$
\bigtriangledown p + \rho_f\ \dot{\mathbf{u}}, \tag{6}
$$

$$
\frac{1}{c^2}\dot{p} + \rho_f\ \bigtriangledown\{\mathbf{u}\}, \tag{7}
$$

where p is the dynamic fluid pressure (the excess above ambient), c is the wave speed in the fluid, ρ_f is the fluid density, and dots denote partial differentiation with respect to time. At fluid-structure interface, momentum and continuity are considered by taking

$$
\frac{\partial p}{\partial n} = -\rho_f\ \ddot{\mathbf{u}}_n \tag{8}
$$

where n is the normal and $\ddot{\mathbf{u}}_n$ denotes the normal component of fluid particle acceleration.

For time-harmonic excitation, the momentum and continuity equations, Eqs. (6, 7), becomes the Helmholtz equation (Everstine, 1997):

$$
\bigtriangledown^2 p + \frac{1}{c^2}\ \ddot{p} = 0, \tag{9}
$$

where $\bigtriangledown^2$ is the Laplacian operator.

The fluid can be modeled with finite element method. Element equations can be derived form Galerking's method formulated as follows

$$
[\mathbf{H}]\{p\} + \rho_f\,[\mathbf{L}]^T\{\ddot{\mathbf{u}}_n\} = 0, \tag{10}
$$

where the terms in the matrices $\mathbf{H}$ and $\mathbf{L}$ are given by

$$
h_{ij} = \int_\Gamma \left[\frac{\partial\psi_i}{\partial x}\frac{\partial\psi_j}{\partial x} + \frac{\partial\psi_i}{\partial y}\frac{\partial\psi_j}{\partial y} + \frac{\partial\psi_i}{\partial z}\frac{\partial\psi_j}{\partial z}\right] d\Gamma, \tag{11}
$$

$$
l_{ij} = \frac{1}{c^2}\int_\Gamma \psi_i\psi_j d\Gamma, \tag{12}
$$

where Γ is the domain of an element of fluid, and ψ_i is the element shape function associated with grid point i.

The coupled solution can be derived combining structure displacement, Eq. (1), with fluid-structure formulation, Eq. (10), and becomes

$$
\begin{bmatrix} [M] & [0] \\ \rho_f[L]^T & [0] \end{bmatrix}\begin{Bmatrix} \{\ddot{\mathbf{X}}\} \\ \{p\} \end{Bmatrix} + \begin{bmatrix} [K] & -[L] \\ [0] & [H] \end{bmatrix}\begin{Bmatrix} \{\mathbf{X}\} \\ \{p\} \end{Bmatrix} = \begin{Bmatrix} \{\mathbf{F}(t)\} \\ \{0\} \end{Bmatrix} \tag{13}
$$

Finally, the effect of fluid pressure on the structure is imposed as a load, applied to the structure, and the structural displacements, derived from Eq. (13), can be calculated from

$$
([\mathbf{M}] + [\mathbf{M_a}])\{\ddot{\mathbf{X}}(t)\} + [\mathbf{K}(\mathbf{N})]\{\mathbf{X}(t)\} = \mathbf{Q}(t), \tag{14}
$$

$$[\mathbf{M}_a] = \rho_f \, [\mathbf{L}] \, [\mathbf{H}]^{-1} \, [\mathbf{L}] \, , \tag{15}$$

where M is structural mass matriz, Eq. (5), and M_a is the so-called *added-mass*, representing inertial effects derived by the presence of the fluid (the mass of the displaced fluid).

Considering interface elements, needed to connect fluid elements to structural elements, as discribed in Pavanello (1991), the matrices $\mathbf{H}$ and $\mathbf{L}$ can be derived:

$$[H] = \frac{a \times b \times t}{45} \begin{bmatrix} 52 & -37 & 45/2 & -23 & 23 & -23 & 45/2 & -37 \\ & -104 & -37 & 0 & -23 & 16 & -23 & 0 \\ & & 52 & -37 & 45/2 & -23 & 23 & -23 \\ & & & 104 & -37 & 0 & -23 & 16 \\ & & & & 52 & -37 & 45/2 & -23 \\ & & & & & 104 & -37 & 0 \\ & & & & & & 52 & -37 \\ sim & & & & & & & 104 \end{bmatrix} , \tag{16}$$

$$[L] = \frac{a \times t}{120} \begin{bmatrix} 37 & 5a & 8 & -4a & 5 & a \\ 28 & -6a & 104 & 0 & 28 & -6a \\ -5 & -a & 8 & 4a & 37 & -5a \end{bmatrix} , \tag{17}$$

where a, b and t are lengths of a fluid element; and ξ and η are its dimentionless lengths, represented in Fig. (2).

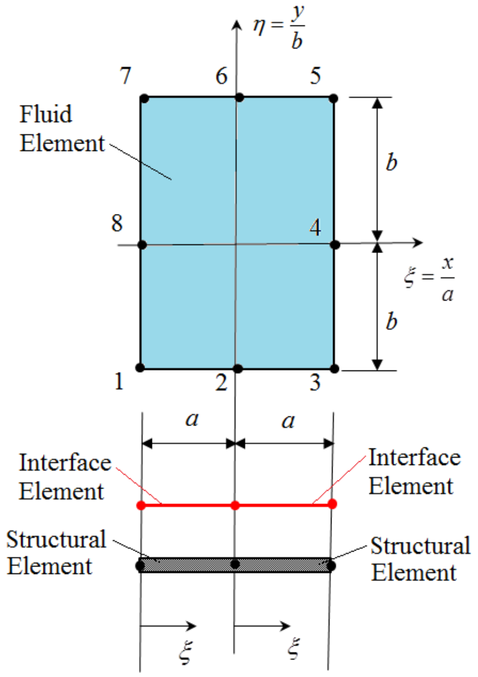

Figure 2. Fluid-Structure grid interface.

From equation of motion, Eq. (14), the following eigenvalue problem can be derived:

$$[\mathbf{K}(\mathbf{N}) - \lambda(\mathbf{M} + \mathbf{M}_a)]\mathbf{Y} = 0, \tag{18}$$

where $\lambda = \omega^2$ are the natural frequencies of the structure (the eigenvalues), and $\mathbf{Y}$ is the eigenvector (the mode shape).

The matrix form of the frequency response functions is calculates as

$$\mathbf{W}(\Omega) = \left[\mathbf{K}(\mathbf{N}) - \Omega^2(\mathbf{M} + \mathbf{M}_a)\right] , \tag{19}$$

where Ω is the excitation frequency.

The equations above show the correlation between dynamic responses and axial load applyed to the coupled solution. Considering the influence exerted by the external loading on the dynamical resonse of the system, it is possible to obtain information about the loading distribution, through an inverse problem approach.

3. Deterministic approach

In the present work, axial force identification is dealt with by formulating a constrained optimization problem, in which ones aim to minimize the cost function, defined as the difference between the values of the experimental data (the natural frequencies of the structure) and those predicted by the Finite Element Model adopted,

$$\mathbf{J} = \sum_{i=1}^{n} \mathbf{W}_p |\omega^{(m)} - \omega^{(c)}(p)|, \tag{20}$$

where $\omega^{(m)}$ is the measured data, $\omega^{(c)}$ designate the calculated values of the natural frequencies, W_p are user-defined weighting factors (in this work, $W_P = 1$), and n is the number of natural frequencies used for identification. In order to deal with imprefection on experimental boundary conditions, the model used is a beam supported at its ends, as shown in Fig. (3). Therefore, the paremeters p include the translational spring constants k_t, the rotational spring constants K_r, and the axial load N.

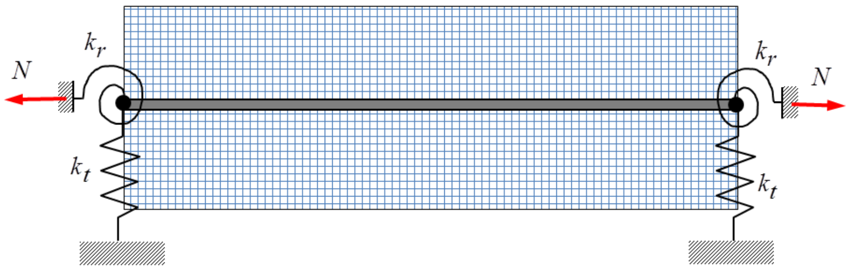

Figure 3. A submerged beam with translational and rotational spring supports.

3.1 Differential Evolution algorithm

Genetic algorithm (GA) is an optimization algorithm based on biological evolution. It is based on Darwin's theory of survival and evolution of species (Michalewicz, 1994; Haupt and Haupt, 1998). The algorithm starts from a population of radom individuals, where an individual is a vector composed with proposal values to the parameters to be optimized, and a population is viewed as a candidate solution to the problem. During the evolutionary process, individuals are gerated, modified from the olders by mutation and crossover process, that mimics the correspondent biological processes; some of the individuals are preserved while others are discarted, after being evaluated with respect to its adaption capability to the environment. The entire process is repeated until a satisfactory solution is found. This class of optimization algorithms have been increasingly applied in solving complex problems due to its robustness and adaptability (Flores *et al.*, 2007).

In the present work, Differential Evolution (DE) is used to solve the optimization problem. DE is a stochastic optimization method, like GA, introduced by Storn and Price (1997), that is able to optimize non-differentiable, nonlinear and multimodal objective functions, which are function of discrete variables. Other capabiblities of this algorithm are: ease of use, good convergence properties (assures global convergence), and parallelizability (to cope with computation intensive cost objective Storn and Price (1995)).

Using DE, the initial vector popoulation should cover the entire parameter space, and assume a uniform probability distribution. In other words, in the initial population, the candidate solution, in generation $G = 0$, is a multidimentional vector

$$V_G = \{\mathbf{p}^l_{i,G}\}^T, i\text{=1,2,...,N}, \text{ where} \tag{21}$$

$$\mathbf{p}^l_{i,G} = S_l(p_i) + rand\,[0,1]\,(S_l - S_u)\,, \tag{22}$$

at the iteration l, where S_l and S_u are, respectively, the lower and uper limit space.

DE gerates new individuals (parameter vectors) by adding weighted difference between two population vectors to a third vector, all chosen randomly, defining the mutation operation

$$\mathbf{p}^l_{i,G+1} = \mathbf{p}^l_{r1,G} + f \cdot \left(\mathbf{p}^l_{r2,G} - \mathbf{p}^l_{r3,G}\right), \tag{23}$$

with random indexes $r1, r2, r3 \in 1, 2, ..., N$, integer, mutually different and $F > 0$. Thus, the mutated vector's parameters are then mixed with the parameters of a third predetermined vector, the so-called *trial vector*, the target vector, as ilustrated in Fig. (4).

Crossover operation is introduced in order to increase the diversity of the perturbed parameter vectors, as described in Storn and Price (1997). Finally, in the end of algorithm loop, the selection process is done comparing the trial vector $p^l_{i,G+1}$ to the target vector $p^l_{i,G}$, using the greedy criterion, with respect to the function to be optimized, Eq. (20).

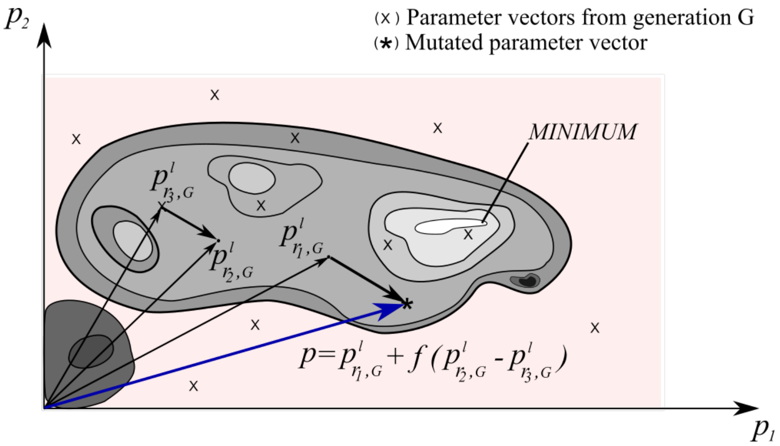

Figure 4. Differential Evolution: representation of two dimentional cost function and mutation operation.

4. Bayesian approach

A Bayesian inference approach is used in the present work in order to solve the optimization problem, as a statistical inference. In this way, the solution of the inverse problem takes a form of a posterior probability distribution $p(\theta|\mathbf{y})$, denominated the conditional probability distribution of the unknown parameters given a set of measurements of outputs $\mathbf{y}$ (experimental data). Using this approach, both predicted and observed quatities are regarded as random variables. From this point of view, experimental uncertainties are directly associated to randomness. Hence, Bayes' theorem for conditional probabilities (the posterior probability distribution) can be written as

$$p\left(\theta|\mathbf{y}\right) = \frac{p\left(\mathbf{y}|\theta\right)p\left(\theta\right)}{p\left(\mathbf{y}\right)}, \tag{24}$$

where $p\left(\mathbf{y}|\theta\right)$ denotes the likelihood function, which corresponds to the conditional probability of the observed data given a set of input, $p(\mathbf{y})$ denotes the marginal probability distributio of the observed data, and $p(\theta)$ denotes the prior probability distribution. The prior probability distribution constains all information about the distribution of θ before doing any measurements. The likelihood represents the probability distribution of the difference between output model predictions, and observed data.

The marginal probability distribution of the observed data may be regarded as a normalization constant,

$$p(\mathbf{y}) = \int_D p(\mathbf{y}|\theta)\ p(\theta)\ d\theta, \tag{25}$$

such that Bayes' theorem may be rewritten as

$$p(\theta|\mathbf{y}) \propto p(\mathbf{y}|\theta)p(\theta), \tag{26}$$

designated as the unnormalizes posterior probability distribution. The basic idea of the Bayesian inference is that one uses Baayes' theorem to convert an *a priori* probability distribution for the parameters θ into a posterior distribution having seen the measurements $\mathbf{y}$. Thus, using Bayesian inference approach, ones aim to know the posterior probability distribution.

Unfortunately, in most cases, prior distributions aren't available, and non-informative prior distributions, such as uniform distribution over θ and D, are commonly enforced. However, if additional information about the distribution of θ is available, it would be incorporated into the prior distribution.

Denoting by $\tilde{\mathbf{y}}$ an unobservable quantity of interest different from the outputs $\bar{y}$, its posterior probability distribution may be computed as

$$p(\tilde{\mathbf{y}}|\mathbf{y}) = \int_D p(\tilde{\mathbf{y}}|\theta)\ p(\theta|\mathbf{y})\ d\theta \tag{27}$$

where the probability distribution $p(\tilde{\mathbf{y}}|\theta)$ may be obtained from uncertainty propagation (Matt and Castello, 2011).

4.1 Markov chain Monte Carlo Sampling

In general, posterior probability is analitically intractable, and the prior probability distribution $p(\theta)$ may be nonstandard. In these situations, inference about the unknown parameters may be treated by simulation.

The Markov Chain Monte Carlo (MCMC) sampling was proposed by Hastings (1970) as a means of drawing samples from Bayes'theorem, Eq. (24), directly, without having to integrate it. MCMC algorithm build a Markov chain for each unknown parameters, such that samples from the chain are samples from the desired posterior distribution.

A widely used Markov chain sampling method is referred to as the Metropolis-Hastings (MH) algorithm (Gilks *et al.*, 1996; Gelman *et al.*, 2003). In the current work, the Metropolis-Hastings algorithm with a uniform distribution is employed to estimate the posterior state-space, using the pseudo-code steps described in Matt and Castello (2011).

5. Results and Discussion

5.1 Physical system

In the present work one aims to determine the axial load applied to piping system used in oil industries. For validating the metodology, an experimental bench has been designed and built, consisting in a reservoir inside which a tubular stainless steel beam, with diameter $\phi = 33.4$ mm, tichness $e = 1.65$ mm as shown in Fig. (5).

Especial fixtures were designed so that the beam-like structure was supported at both ends for two different boundary conditions: pinned-pinned (PP) and clamped-clamped (CC) conditions. The effective length of the tube, between the fixtures is $L = 4.0$ meters.

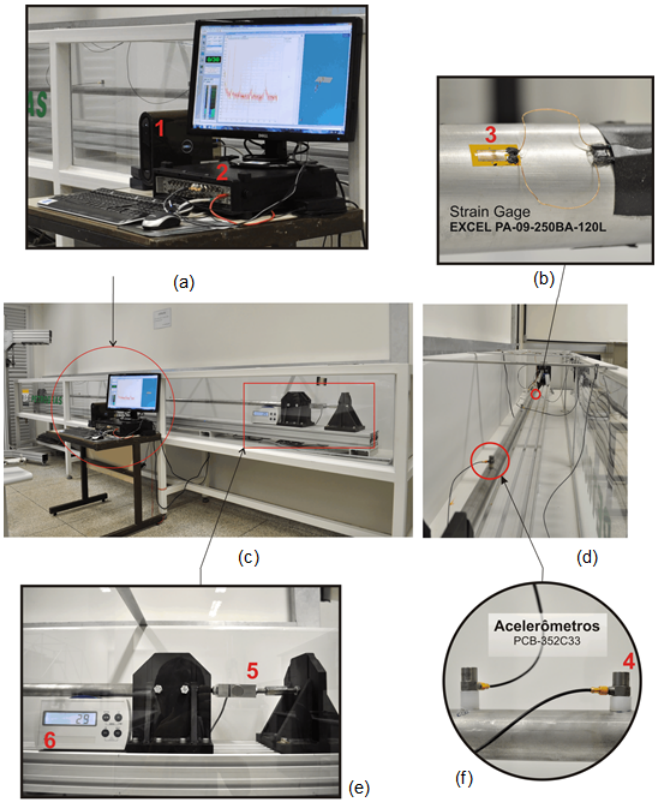

Figure 5. Experimental bench: (a) data acquisiton system; (b) detail of strain-gauges fixed in tubular beam; (c) overview of the experimental bench; (d) side-view; (e) fixtures used to control axial loads; (f) accelerometers fixed over the beam.

As discussed in Section 2, the experimental data of interest in the present work are the natural frequencies of the structure. For this purpose, some Experimental Modal Analysis (EMA) techniques have been used to determine the experimnetal natural frequencies, but will not be discussed here.

5.2 DE results

In order to analyze effect of individual components of the experimental bench, numerous scenarios have been considered. Initially, the effect of boundary conditions on natural frequencies was examined. In this case, EMA procedures were done without the presence of water, for the two conditions: CC and PP. In these situations, natural frequencies were obtained for diferet levels of axial load, presented in Tab. (1,2).

About the results, one can conclude that the axial load changes the response of the mechanical systems. The changes are substantial and proportional to the level of load. Furthermore, in CC condition natural frequencies are higher, if compared with the PP conditions, as predicted by theory, once the structure has a higher stiffness.

Table 1. EMA analysis for PP beam, without FSI effect.

Frequency (Hz)	$P = 1000N$	$P = 2000N$	$P = 3000N$	$P = 4000N$	$P = 5000N$
f_1	8.091	9.340	10.189	10.214	10.993
f_2	24.246	26.532	27.885	27.887	29.086
f_3	51.459	53.969	55.483	55.485	56.895
f_4	90.281	92.705	95.501	94.678	95.887
f_5	138.02	140.53	142.31	142.32	143.97

Table 2. EMA analysis for CC beam, without FSI effect.

Frequency (Hz)	$P = 1000N$	$P = 2000N$	$P = 3000N$	$P = 4000N$	$P = 5000N$
f_1	12.489	12.868	13.370	13.941	14.307
f_2	33.919	34.431	35.125	35.915	35.916
f_3	64.981	65.377	66.051	66.952	68.107
f_4	107.760	107.910	108.170	109.490	70.883
f_5	153.97	153.90	159.53	157.63	111.07

For evaluation of FSI effects, the structure was tested submerged in water. For this analysis, Tab. 3 and 4 shown the tests includind FSI conditions. The results show the effect of added-mass, changing the frequencies to low values, if compared with results presented in tab. 2 and tab. 1.

Table 3. EMA analysis for PP beam, with FSI effect.

Frequency (Hz)	$P = 1000N$	$P = 2000N$	$P = 3000N$	$P = 4000N$	$P = 5000N$
f_1	5.5571	6.3342	6.9915	7.6288	8.2417
f_2	18.408	19.356	20.304	22.155	23.935
f_3	39.405	40.565	41.530	42.604	43.652
f_4	69.145	70.337	71.398	72.560	73.792
f_5	106.33	107.64	108.79	109.90	111.10

Table 4. EMA analysis for CC beam, with FSI effect.

Frequency (Hz)	$P = 1000N$	$P = 2000N$	$P = 3000N$	$P = 4000N$	$P = 5000N$
f_1	9.2994	9.7357	10.1269	10.5180	10.9380
f_2	25.483	26.039	26.5975	27.156	27.838
f_3	48.782	49.374	49.934	50.684	51.430
f_4	81.568	82.082	82.555	83.504	84.279
f_5	120.33	121.07	121.65	122.68	123.68

The same results are presented in fig. (6), that show the linear relation between tha axial load P and experimental frequencies Ω, as one might expect, predicted by Bahra and Greening (2009).

Admiting the linearity of the stress-stiffening effect, from Fig. (6) it is possible to note that PP conditions are more susceptible to manufacturing, assembly, and other experimental conditions. Moreover, analysing the experimental bench design, was noted that the PP condition was susceptible by the axial load and uncertainties.

With intent to minimize the errors, in PP conditions the tortional springs were considered in the computational model, as ilustrated in Fig. (3). The deterministic updating procedure was applied using the tortional spring as updating parameters to minimise the differences in the natural frequencies and obtained the spring constant $K_t = 3.5076 \times 10^6$ N/rad. The tortional spring is considered only for PP condition.

Under these circumstances the Differential Evolution (DE) algorithm was applied using the axial load as updating parameters, and the dynamically identified loads compared with those measured independently with a cell load. Table 5 shows the dynamically identified loads, including the tortional spring effect $P*$, and without the spring P, compared with those measured independently. Analyzing these results one can conclude that other effects than the influence of boundary conditions influence the problem.

On the other hand, a close match of the axial load is seen to be obtained considering CC condition, as shown in Tab. 6. However, it is observed that in all situations the error is bigger for low values of axial load. It could still be argued that

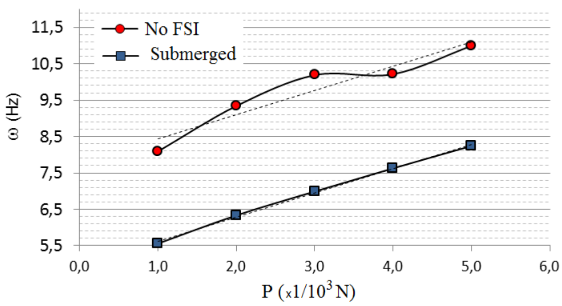

(a)

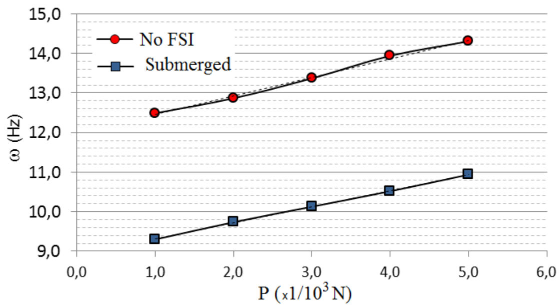

(b)

Figure 6. EMA results for the first natural frequency, f_1: (a) PP boundary condition; (b) CC boundary conditions

Table 5. Deterministic identification: PP condition and without FSI effects.

Expected value	Submerged [*Error (%)*]	no FSI [*Error (%)*]
1.000	3117,1 [*211, 7*]	428,93 [*57, 1*]
2.000	4883,8 [*144, 2*]	2.224,2 [*11, 21*]
3.000	6.230,9 [*107, 7*]	9.592,4 [*219, 7*]
4.000	6.272,3 [*56, 8*]	3.634,5 [*9, 14*]
5.000	7.615,7 [*52, 3*]	4.998,6 [*0, 0*]

for low values of axial load, stress-stiffening effect has low level of contribution to change the dynamical response of the system; random and others effects, as neglected effects (e.g., gravity), have similar contribution.

Table 6. Deterministic identification: CC condition and without FSI effects.

Expected value	P	Error (%)
1.000	1.305,2	30,5
2.000	1.984,3	0,8
3.000	2.918,3	2,7
4.000	4.028,9	0,7
5.000	4.767,9	4,6

To this extent the results provide some confidence that finite element model combined with DE updating will become viable tool in practical situations

5.3 MCMC results

With intent to account the presence of uncertainties in the experimental data, presented above, MCMC procedures were used assuming uncorrelated errors ν_i, $i = 1, 2, ..., N_y$, that are considered to be additive, with zero means, so that the components of observed data vector are given by

$$\mathbf{y}_i = \overline{\mathbf{y}}_i + \nu_i, \quad i\text{=1,2,...,}N_y. \tag{28}$$

Considering only uncorrelated erros, with Gaussian distribution, hence the likelihood function becomes

$$p(\mathbf{y}|\theta) \propto \frac{1}{(\sigma^2)^{N_y/2}} \, exp\left\{-\frac{1}{2\sigma^2}[\mathbf{y} - \overline{\mathbf{y}}(\theta)]^T[\mathbf{y} - \overline{\mathbf{y}}(\theta)]\right\}, \tag{29}$$

For Bayesian inference approach, one assumes known known constant variance σ^2 (considering 2% of error for FRF measurements, in EMA procedures), and results for the updated axial forces are indicated in Fig. (7).

Considering FSI conditions, marginal posterior distributions for axial load were derived from point estimates using MCMC. Figures 8 and 9 plots histograms to the posteior marginal probability distributios for axial force, considering FSI effect.

Results shown that the posterior state space exploited using Markov chain Monte Carlo (MCMC) algorithms, is able to estimates of the statistics of the unknown axial loads, for all situations presented above. Quite accurate estimates as well as low variances were obtained for the axial load, due to the sensitivity of the chosen observed data with respect to that parameter

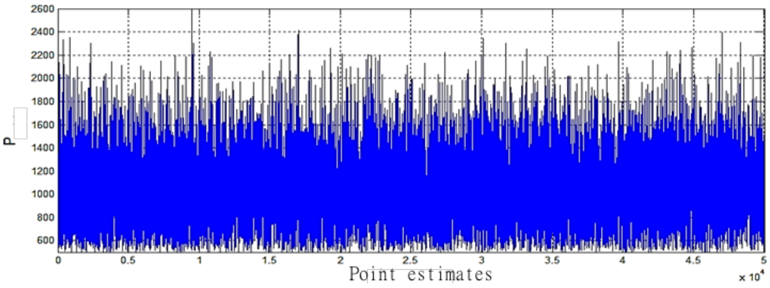

Figure 7. Point Estimates of axial load for PP conditions, without FSI effects, comprising 50,000 data points.

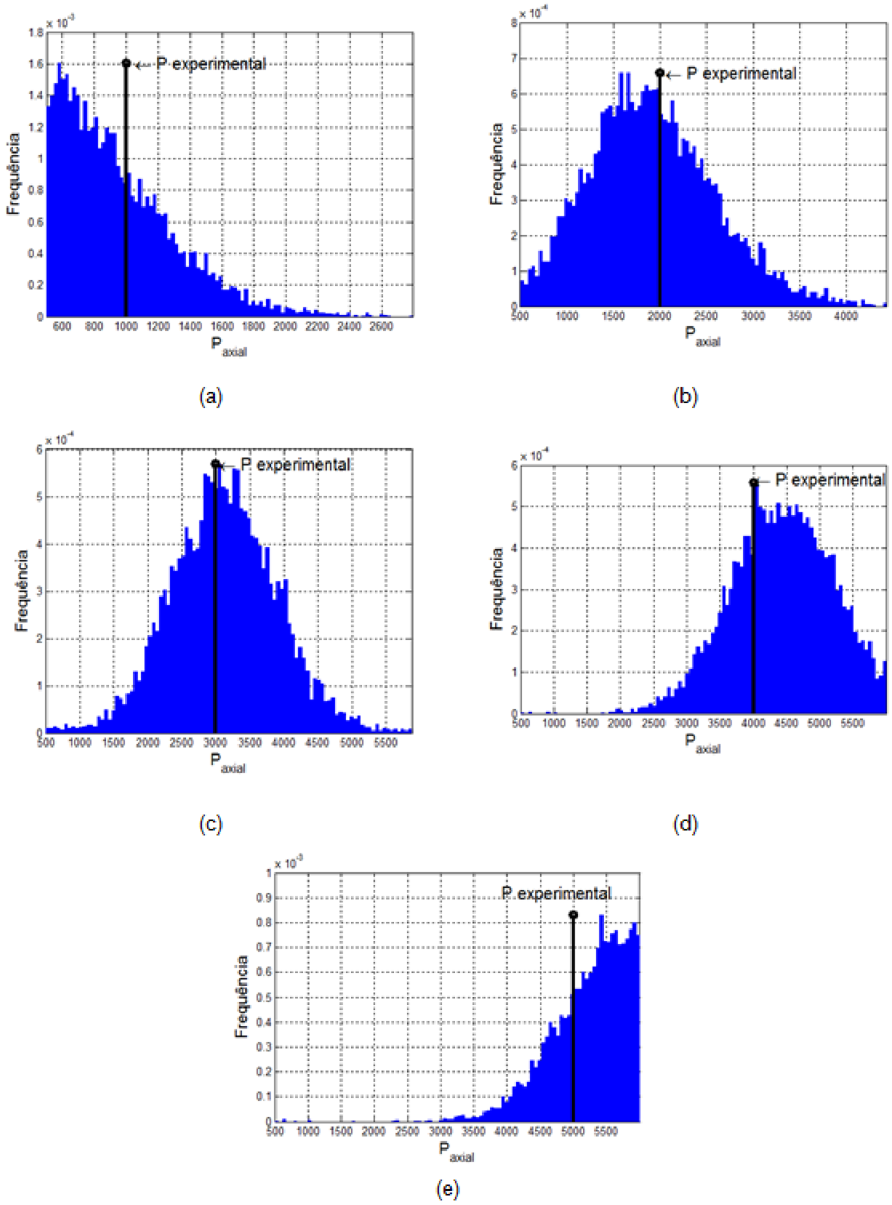

Figure 8. Posterior distribution for axial load, with PP conditions and including FSI effects.

6. ACKNOWLEDGEMENTS

Mr. Kitatani Jr. is thankful to FAPEMIG for his Ph.D. scholarship. Dr. Rade acknowledge CNPq for his research grants. The authors also acknowledge PETROBRAS for financing of the present research work.

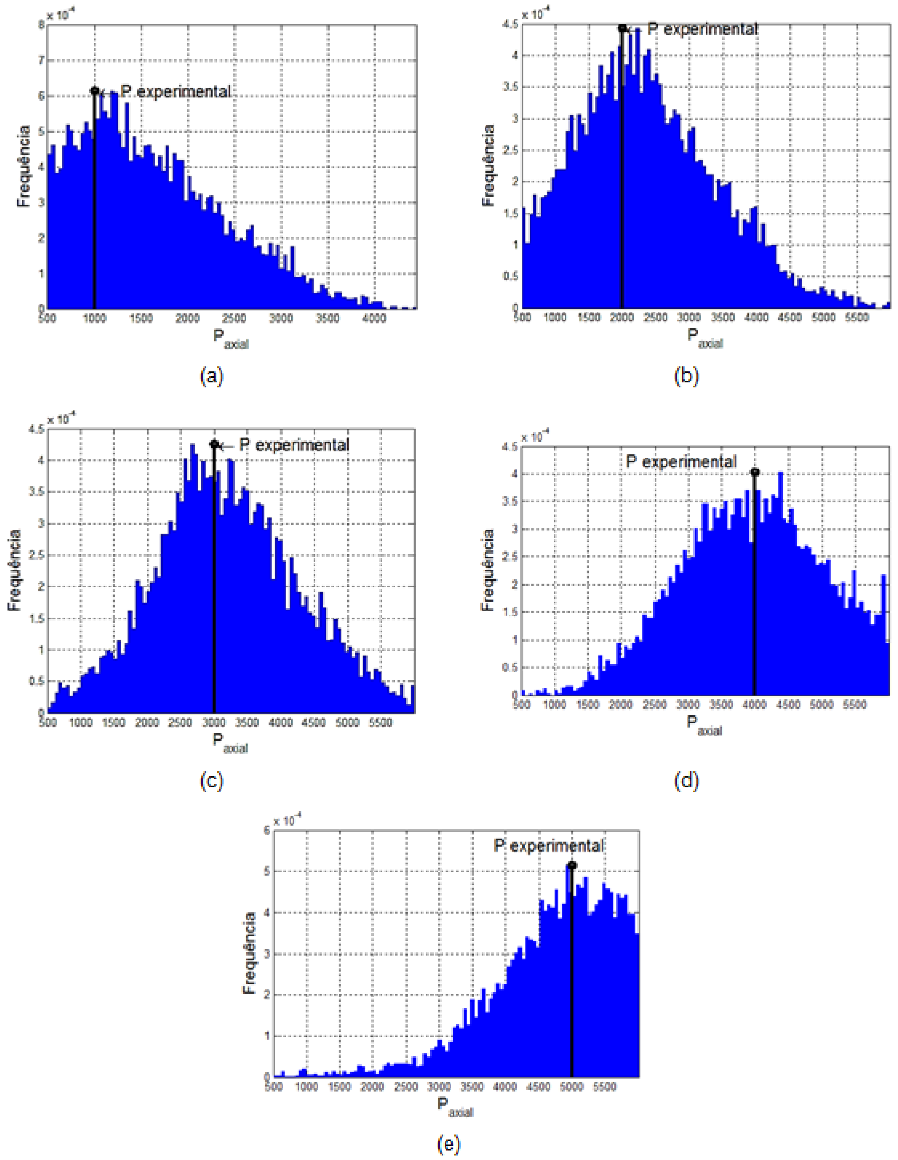

Figure 9. Posterior distribution for axial load, with PP conditions and including FSI effects.

7. REFERENCES

Bahra, A.S. and Greening, P.D., 2009. "Identifying axial load patterns using space frame fems and measured vibration data". *Mechanical Systems and Signal Processing*, Vol. 23, p. 1282âĂŞ1297.

Craig Jr, R.R., 1981. *Structural Dynamics: An Introduction to Computer Methods*. John Wiley & Sons, New Jersey, 1st edition.

Craig Jr, R.R. and Kurdila, A.J., 2006. *Fundamentals of Structural Dynamics*. John Wiley & Sons, New Jersey, 2nd edition.

Everstine, G.C., 1997. "Finite element formulations of structural acoustic problems". *Computer and Structure*, Vol. 65, pp. 307–321.

Felippa, C.A. and Geers, T.L., 1988. "Partitioned analysis of coupled mechanical systems". *Engineering Computations*, Vol. 5, p. 123âĂŞ133.

Felippa, C.A. and Park, K.C., 2006. *Engineering Structures under Extreme Conditions*. IOS Press, Amsterdam.

Felippa, C.A. and Park, K.C., 2008. *Computational Aspects of Structural Dynamics and Vibrations*. Springer-Verlag, Berlin.

Flores, J.E.R., 2004. *Caracterização do Efeito de Enrijecimento por Tensões e Identificação de Cargas em Estruturas Baseadas em Respostas Dinâmicas*. Ph.D. thesis, Universidade Federal de Uberlandia, Brazil.

Flores, J.E.R., Vianna, F.A.C., Rade, D.A. and Steffen Jr, V., 2007. "Identification of external forces in mechanical systems by using lifecycle model and stress-stiffening effect". *Mechanical Systems and Signal Processing*, Vol. 21, pp. 2900–2917.

Gelman, A., Carlin, J.B., Stern, H.S. and Rubin, D.B., 2003. *Bayesian data analysis*. Chapman & Hall, Boca Raton, 2nd edition.

Gilks, W.R., Richardson, S. and Spiegelhalter, D.J., 1996. *Markov Chain Monte Carlo in Practice*. Chapman & Hall, London, 1st edition.

Greening, P.D. and Lieven, N.A.J., 1999. "Modelling dynamic response of stresses structures". In *Proceedings of the 17th International Modal Analysis Conference*. Florida, USA.

Hastings, W.K., 1970. "Monte carlo sampling methods using markov chains and their applications". *Biometrika*, Vol. 57(1), pp. 97–109.

Haupt, R.L. and Haupt, S.E., 1998. *Practical Genetic Algorithm*. Wiley-Interscience, New York, 1st edition.

Livingston, T., Béliveau, J.G. and Huston, D.R., 1995. "Estimation of axial load in prismatic members using flexural vibration". *Journal of Sound and Vibration*, Vol. 179, pp. 899–908.

Matt, C.F. and Castello, D.A., 2011. "A bayesian inference approach to estimate elastic and damping parameters of a structure subjected to vibration testes". In *Proceedings of the XIV International Symposium on Dynamic Problems of Mechanics - DINAME2011*. São Sebastião, Brazil.

Michalewicz, Z., 1994. *Genetic Algorithms + Data Structures = Evolution Programs*. Springer, New York, 2nd edition.

Pavanello, R., 1991. *Contribution a l'Etude Hydroelastique des Structures a Symetrie Cyclique*. Ph.D. thesis, Institut National des Sciences Appliquees de Lyon, Insal.

Storn, R. and Price, K., 1995. "Differential evolution - a simple and efficient heuristic for global optimization over continuous spaces". Technical Report TR-95-012, ICSI.

Storn, R. and Price, K., 1997. "Differential evolution - a simple and efficient heuristic for global optimization over continuous spaces". *Journal of Global Optimization*, Vol. 11, pp. 341–359.

8. RESPONSIBILITY NOTICE

The authos are the only responsible for the printed material included in this paper.